Numerical Analysis of Wave and Hydrodynamic Models for Energy Balance and Primitive Equations

Worachat Wannawong*, Usa W. Humphries, Prungchan Wongwises,
Suphat Vongvisessomjai and Wiriya Lueangaram

Abstract—A numerical analysis of wave and hydrodynamic models is used to investigate the influence of WAve and Storm Surge (WASS) in the regional and coastal zones. The numerical analyzed system consists of the WAve Model Cycle 4 (WAMC4) and the Princeton Ocean Model (POM) which used to solve the energy balance and primitive equations respectively. The results of both models presented the incorporated surface wave in the regional zone affected the coastal storm surge zone. Specifically, the results indicated that the WASS generally under the approximation is not only the peak surge but also the coastal water level drop which can also cause substantial impact on the coastal environment. The wave–induced surface stress affected the storm surge can significantly improve storm surge prediction. Finally, the calibration of wave module according to the minimum error of the significant wave height (Hs) is not necessarily result in the optimum wave module in the WASS analyzed system for the WASS prediction.

Keywords—energy balance equation, numerical analysis, primitive equation, storm surge, wave.

I. INTRODUCTION

Numerous efforts have been carried out for the theoretical analysis and numerical modeling of the WAve and Storm Surge (WASS) induced by hurricanes, cyclones and typhoons in the global, regional and coastal scales [18]. In recent year, most studies have been focused on the individual phenomena and characteristic of storm waves, tides, surges and currents [25], [27], [26], [33] which were accepted and applied in the numerical analysis of wave and hydrodynamic models [34], [35].

Brikshavana and Luadsong [28] studied the splitting modified donor–cell schemes to solve the spectral action balance equation in the Simulating WAves Nearshore (SWAN) model [16]. The SWAN model is a third generation wave model developed by Booij et al. [16] in the spirit of the WAve Model (WAM) [21]. In early stage of studies, a third generation WAve Model Cycle 4 (WAMC4) is based on Eulerian formulation of the discrete spectral balance of action density that accounts for refractive propagation over arbitrary bathymetry and current fields [7], [4], [9]. The WAMC4 model has been used in the Gulf of Thailand (GoT) by the Thai Meteorological Department and Royal Thai Navy since 1997. The ocean waves generated by strong winds during the passages of Typhoons Vae in 1952 and Linda in 1997 were studied by using the WAMC4 model [25]. Vongvisessomjai [26] reported

that the characteristics of typhoons became more interesting. The disasters can be alleviated from the understanding of tropical cyclone characteristics through the proper warning before entering into the GoT.

For the hydrodynamic model, the Princeton Ocean Model (POM) described by Blumberg and Mellor [1] has been simulated to study the external gravity waves, internal gravity waves, tidal waves, surges and currents. The POM model has been used to study the currents in the GoT by the Royal Thai Navy since 2000 and it was also developed by the Thailand Research Fund in 2003 in order to study the storm–surge and the effect of tidal forcing. Aschariyaphota et al. [15] studied the seasonal circulations and thermohaline variabilities by using the orthogonal curvilinear grid in the horizontal coordinates. Their results were reported that the effects of wind forcing with open boundary condition were found to be important for seasonal circulations. The report of Wannawong et al. [33] showed the comparison of orthogonal curvilinear grid and orthogonal rectangular grid in the horizontal coordinates and was found that although the orthogonal curvilinear grid provided more acceptable velocity of sea water current in the coastal area than the orthogonal rectangular grid, the velocities of current from both grids were not much different. The orthogonal rectangular grid, therefore, was used to study the storm surge case in the present study.

The objective of this work was to investigate the influence of WASS in the regional and coastal zones by the numerical analysis of wave and hydrodynamic models under typhoon wind and pressure forcing during the passage of Typhoon Linda 1997 (Fig. 1). A brief description of the numerical analyzed models used in the WASS analyzed system is provided in Section II. Section III introduces the model parameters and the numerical experiments performed. The results of WASS analyzed system in regional zone which affected the coastal storm surge zone are presented in Section IV, followed by conclusion and discussions in Section V.

II. DESCRIPTION OF NUMERICAL ANALYZED MODELS

The numerical analysis of wave and hydrodynamic models are called as the WAve and Storm Surge (WASS) model. The WASS model consists of the WAve Model Cycle 4 (WAMC4) [21], [7], [4] and the Princeton Ocean Model (POM) [1] which used to solve the energy balance and primitive equations respectively. The WASS model has been developed in order to simultaneously calculate an arbitrary number of sub–domains under the atmospheric forcing at the boundary conditions. The

WASS model for energy balance and primitive equations is described firstly and the numerical process is presented later.

A. *The wave model for the energy balance equation*

The WAMC4 model solves the energy balance equation in the regional scale with the terms of the discrete energy density[1], $F(\theta, f; \mathbf{x}, t)$, where t represents time, $\mathbf{x}$ represents the geographical space in spherical coordinates (λ, ϕ), and (θ, f) represent the spectral space (direction and frequency, respectively). The wave direction θ represents the wave direction measured clockwise from the true north. Excluding the intrinsic frequency, σ, as a coordinate allows the model to overcome the problem of high frequency waves propagating on strong opposite currents (e.g. the absence of diffraction and currents for the coastal scale).

The governing equation of the WAMC4 model on the spherical coordinates (λ, ϕ) reads,

$$\frac{\partial F}{\partial t} + \frac{\partial c_{g,\lambda} F}{\partial \lambda} + (\cos \phi)^{-1} \frac{\partial c_{g,\phi}(\cos \phi) F}{\partial \phi} + \frac{\partial c_\theta F}{\partial \theta} = S_{tot} \quad (1)$$

where the propagation speed in the different spaces; $c_{g,\lambda}, c_{g,\phi}$, and c_θ are given by [20], [8],

$$c_{g,\lambda} = \dot{\lambda} = \frac{d\lambda}{dt} = (c_g \sin \theta)(R \cos \phi)^{-1}, \quad (2)$$

$$c_{g,\phi} = \dot{\phi} = \frac{d\phi}{dt} = (c_g \cos \theta)R^{-1}, \quad (3)$$

$$c_\theta = \dot{\theta} = \frac{d\theta}{dt} = (c_g \sin \theta \tan \phi)R^{-1}. \quad (4)$$

Here $c_g = g/2\omega = g/2(2\pi f) = g/4\pi f$ denotes the group velocity of the deep water condition, g represents the gravitational acceleration, ω represents the angular frequency, f represents the frequency, and R represents the radius of the earth. The detail of wave group on the spherical coordinates is shown in Appendix A.

On the right hand side of the equation (1), S_{tot} is the function representing the source and sink functions, and the conservative non–linear transfer of energy between wave components. For the present applications, the wave model included the standard WAMC4 formulations for the S_{tot} terms; wind input S_{in}, non–linear quadruplet wave–wave interactions S_{nl}, whitecapping dissipation S_{ds}, and bottom friction dissipation S_{bf}. For the complete explanation on the physics included in S_{tot}, the reader is referred to Komen et al. [4] and their references.

The wind input formulation is based on the resonant interaction between the wave induced pressure fluctuations and the waves of Miles' theory. This source of energy is represented as,

$$S_{in} = \gamma F \quad (5)$$

where γ is the growth rate of the waves, also called Miles' wave growth mechanism. In the WAMC4 model, this term

---

[1] It is worth remarking that the letter F denotes the discrete representation of the wave energy density, E.

is based on the theory proposed by Janssen [17]. According to Janssen [17], the interphase atmosphere–ocean represents a coupled system where the growth rate of waves depends on the wind, whose profile depends on the sea state. The term γ is expressed as below in the WAMC4 model.

$$\gamma = \max \left[0, (\rho_a/\rho_w)\beta X^2 \right] \quad ; \quad X = (u^*/c)\cos \vartheta, \quad (6)$$

where ρ_a is the density of air, ρ_w is the density of sea water, ϑ is the relative direction between wind and waves, $u^* = \sqrt{\tau/\rho_a}$ is the friction velocity where τ is the wind stress, c is the phase velocity of the waves, and β is the Miles' parameter given by,

$$\beta = (1.2/\kappa^2)\nu \ln^4 \nu \quad ; \quad \nu = \frac{gz_e}{(\kappa c_p)^2} \exp(\kappa/X). \quad (7)$$

where z_e represents the effective roughness length, c_p is the wave propagation speed and $\kappa = 0.41$ is the von Kármán constant. The nonlinear resonant interaction between the quadruplet of wave components is included in the WAM through an approximation to the exact expression,

$$S_{in}^{exact}(\mathbf{k_4}) = \int \omega_4 \varsigma \delta(\mathbf{k}_1 + \mathbf{k}_2 - \mathbf{k}_3 - \mathbf{k}_4)\delta(\omega_1 + \omega_2$$
$$-\omega_3 - \omega_4) \times [n_1 n_2(n_3 + n_4)$$
$$-n_3 n_4(n_1 + n_2)]d\mathbf{k}_1 d\mathbf{k}_2 d\mathbf{k}_3 d\mathbf{k}_4 \quad (8)$$

where $n_j = F(k_j)/\omega_j$ is the action density and the coefficient ς is the coupling coefficient. The approximation included in the WAM (DIA method, Hasselmann et al. [22]) reduces the space of resonant quadruplets to a two–dimensional plane where the discrete interaction of a symmetric pair of configurations is only used (see Figs. 3.1 and 3.2 in van Vledder [6]).

On the finite–depth waters, the computation of S_{nl} is carried out in similar way as on the deep waters, but including a scaling factor:

$$S_{nl} = \Upsilon(\bar{k}H)S_{nl} \quad (9)$$

In the equation (9), $\bar{k} = [E_{tot}^{-1} \int F(f,\theta)k^{-1/2}df d\theta]^{-2}$ is the mean of wave number, E_{tot} is the total of wave energy density and the scaling factor Υ reads,

$$\Upsilon(\chi) = 1 + \frac{5.5}{\chi}\left(1 - \frac{5\chi}{6}\right)\exp\left(-\frac{5\chi}{4}\right), \quad (10)$$

with $\chi = (3/4)\bar{k}H$.

The term representing the energy dissipation by wave breaking on the deep waters (also called the whitecapping) is based on the extension of the formulation proposed by Komen et al. [3]. In Komen's formulation, the existence of an equilibrium solution of the energy balance equation during fully developed sea condition is assumed. Once the Janssen's theory for the wave growth by sea–atmosphere coupling was implemented, the Komen's formulation had to be extended in order to obtain the proper balance during fully developed sea conditions. In the WAMC4 model, the term S_{ds} is evaluated as,

$$S_{ds} = -C_{d1}\bar{\omega}\bar{k}^4 E_{tot}^2 \left[(1 - C_{d2})(k/\bar{k}) + C_{d2}(k/\bar{k})^2\right]F \quad (11)$$

where E_{tot} is the total energy, $C_{d1} = 4.5$, and $C_{d2} = 0.5$.

For the shallow water condition, the right hand side of the equation (1) need to be extended to include the additional

source function S_{bf} representing the energy loss due to bottom friction and percolation. The bottom friction dissipation term, S_{bf}, is represented according to the formulation proposed during the Joint North Sea Wave Project (JONSWAP) by Hasselmann et al. [11],

$$S_{bf} = -\frac{\Gamma}{g^2} \frac{\omega^2}{\sinh^2 kD} F \qquad (12)$$

with $\Gamma = 0.038$, ω is the angular frequency ($\omega^2 = gk \tanh kD$), g is the gravitational acceleration, k is the wave number and D is the finite depth dispersion relation.

B. The hydrodynamic model for the primitive equation

The governing equation of the hydrodynamic model can be expressed in the system of orthogonal Cartesian coordinates which consists of the Reynold's averaged equations of mass, momentum, and temperature and salinity conservations. The equations include the effect of the gravitational/buoyancy forces as well as the effect of the Coriolis pseudo–force which are followed in this section.

Continuity equation:

$$\frac{\partial u}{\partial x} + \frac{\partial v}{\partial y} + \frac{\partial w}{\partial z} = 0, \qquad (13)$$

x–momentum equation:

$$\frac{du}{dt} = -\frac{1}{\rho_\circ} \frac{\partial p}{\partial x} + fv + \frac{\partial}{\partial z}(A_{mv} \frac{\partial u}{\partial z}) + F_x, \qquad (14)$$

y–momentum equation:

$$\frac{dv}{dt} = -\frac{1}{\rho_\circ} \frac{\partial p}{\partial y} - fu + \frac{\partial}{\partial z}(A_{mv} \frac{\partial v}{\partial z}) + F_y, \qquad (15)$$

z–momentum or hydrostatic equation:

$$\frac{\partial p}{\partial z} = -\rho g, \qquad (16)$$

Temperature equation:

$$\frac{dT}{dt} = \frac{\partial}{\partial z}(A_{hv} \frac{\partial T}{\partial z}) + F_T, \qquad (17)$$

Salinity equation:

$$\frac{dS}{dt} = \frac{\partial}{\partial z}(A_{hv} \frac{\partial S}{\partial z}) + F_S, \qquad (18)$$

The terms $d(\cdot)/dt$, F_x, F_y, F_T and F_S found in the equations (14), (15), (17) and (18) represent the total derivative terms, these unresolved processes and in analogy to the molecular diffusion can be written as

$$F_x = \frac{\partial}{\partial x}\left[2A_m \frac{\partial u}{\partial x}\right] + \frac{\partial}{\partial y}\left[A_m \left(\frac{\partial u}{\partial y} + \frac{\partial v}{\partial x}\right)\right],$$

$$F_y = \frac{\partial}{\partial y}\left[2A_m \frac{\partial v}{\partial y}\right] + \frac{\partial}{\partial x}\left[A_m \left(\frac{\partial u}{\partial y} + \frac{\partial v}{\partial x}\right)\right],$$

and

$$F_{T,S} = \frac{\partial}{\partial x} A_h \frac{\partial(T,S)}{\partial x} + \frac{\partial}{\partial y} A_h \frac{\partial(T,S)}{\partial y}.$$

where u, v are the horizontal components of the velocity vector, w is the vertical component of the velocity vector, g is the gravitational acceleration, p is the local pressure,

$\rho(x, y, z, t, T, S)$ is the local density, $\rho_\circ$ is the reference water density, A_m is the horizontal turbulent diffusion coefficient, A_{mv} is the vertical turbulent diffusion coefficient, $f = 2\Omega \sin \phi$ is the Coriolis parameter where Ω is the speed of angular rotation of the Earth by $\Omega = 7.2921 \times 10^{-5}\ rad\ s^{-1}$ and ϕ is the latitude, T is the potential temperature, S is the potential salinity, A_h is the horizontal thermal diffusivity coefficient, A_{hv} is the vertical thermal diffusivity coefficient, the terms F_x and F_y are the horizontal viscosity terms and the terms F_T and F_S are the horizontal diffusion terms of temperature and salinity respectively.

The main assumptions used in the derivation of the above equations are that: (a) the water is incompressible ($D\rho/Dt = 0$); (b) the density differences are small and can be neglected, except in buoyant forces (Boussinesq approximation). Consequently, the density $\rho_\circ$ used in the x and y momentum equations (14) and (15) is a reference density that is either represented by the standard density of the water or by the depth averaged water density as follows:

$$\rho_\circ = \frac{1}{\eta + h} \int_{-h}^{\eta} \rho dz = \frac{1}{D} \int_{-h}^{\eta} \rho dz \qquad (19)$$

where the total depth D is expressed as: $D = \eta + h$ that is, the sum of the sea surface elevation η above the mean sea level (MSL) plus the depth h of the still water level. The density ρ used in the z–momentum is represented by the sum of the reference density $\rho_\circ$ and its variation ρ' ($\rho = \rho_\circ + \rho'$). For the last assumption (c), the vertical dimensions are much smaller than the horizontal dimensions of the water field and the vertical motions are much smaller than the horizontal ones. Consequently, the vertical momentum equation reduces to the hydrostatic law (hydrostatic approximation) and the Coriolis term $2\Omega(v \sin \phi - w \cos \phi)$ reduces to $2\Omega v \sin \phi$ (see the equation (14)). The vertical integration of the equation (16) from the depth z to the free surface η yields the pressure at the water depth z as:

$$p|_\eta - p|_z = g \int_z^\eta \rho dz' \longrightarrow$$

$$p = p_{atm} + g\rho_\circ(\eta - z) + g \int_z^\eta \rho' dz' \qquad (20)$$

where z' is a dummy variable for integration, η is the sea surface elevation above the mean sea level (MSL), $p|_z = p = p(x, y, z, t)$ and $p|_\eta = p_{atm}$ is the Standard Atmospheric Pressure.

To close the above system of the continuity and motion equations, it is necessary to state the relationship of the water density, temperature and pressure. This relationship in POM is coded by the following formulation proposed by Mellor [5], that approximates the more general, and also more computationally expensive. The formulation of the International Equation of State (UNESCO) are shown below.

$$\rho(S, T, p) = \rho(S, T, 0) + \frac{p}{c^2}(1 - 0.20\frac{p}{c^2}) \cdot 10^4 \qquad (21)$$

$$c(S, T, p) = 1449.2 + 1.34(S - 35) + 4.55T - 0.045T^2$$
$$+ 0.00821p + 15.0 \cdot 10^{-9}p^2 \qquad (22)$$

where T is the temperature, p is the gage pressure, S is the salinity and c is the speed of sound.

C. Boundary conditions

1) Surface boundary conditions: The continuity, momentum and temperature surface boundary conditions describe the interaction of the water surface with the atmosphere. They are defined as:

$$w|_\eta = \left[\frac{\partial \eta}{\partial t} + u\frac{\partial \eta}{\partial x} + v\frac{\partial \eta}{\partial y}\right]_\eta \quad (23)$$

$$A_{mv}\begin{bmatrix}\partial u/\partial z \\ \partial v/\partial z\end{bmatrix}_\eta = \begin{bmatrix}\tau_{sx}/\rho_\circ \\ \tau_{sy}/\rho_\circ\end{bmatrix} \quad (24)$$

$$\dot{T} = \rho_\circ A_{hv}\frac{\partial T}{\partial z}\bigg|_\eta \quad (25)$$

$$\dot{S} = \rho_\circ A_{hv}\frac{\partial S}{\partial z}\bigg|_\eta \quad (26)$$

The equation (23) represents the surface boundary condition for the continuity equation (13), as expressed by the kinematic free surface condition. At the free surface, the kinematic boundary condition can be derived considering the fact that the free surface is a material boundary for which a particle initially on the boundary will remain on the boundary. Assuming that there is no water penetrating the free surface, then the material or total derivative at the free surface $(\eta - z)$ is zero, therefore:

$$\frac{D(\eta - z)}{Dt} = \frac{D\eta}{Dt} - \frac{Dz}{Dt} = 0 \implies$$

$$\left[\frac{\partial \eta}{\partial t} + u\frac{\partial \eta}{\partial x} + v\frac{\partial \eta}{\partial y} + w\frac{\partial \eta}{\partial z}\right]_\eta - \left[\frac{\partial z}{\partial t} + u\frac{\partial z}{\partial x} + v\frac{\partial z}{\partial y}\right]$$

$$+ w\frac{\partial z}{\partial z}\bigg]_z = 0 \quad (27)$$

Since, $\partial \eta/\partial z = \partial z/\partial t = \partial z/\partial x = \partial z/\partial y = 0$ and $\partial z/\partial z = 1$, the equation (27) reduces to the equation (23).

The equation (24) represents the surface boundary condition for the z–momentum or the hydrostatic equation (16) with the surface wind stresses given by the drag law (bulk formula) as:

$$\begin{bmatrix}\tau_{sx} \\ \tau_{sy}\end{bmatrix} = \rho_{air}C_M W\begin{bmatrix}W_x \\ W_y\end{bmatrix} \;\;; \;\; \tau_s = \rho_{air}C_M|W|W \;\;;$$

$$W = \left(W_x^2 + W_y^2\right)^{1/2} \quad (28)$$

where W is the wind speed at $10\ m$ above the sea water surface, W_x and W_y are the two components of the wind speed vector, ρ_{air} is the density of the air at the standard atmospheric conditions, C_M is the bulk momentum transfer (drag) coefficient and τ_s is the wind imposed surface stress.

The drag coefficient (C_M) is assumed to vary with the wind speed as:

$$10^3 C_M = \begin{cases} 2.5 & \text{if } |W| > 22\ m\ s^{-1} \\ 0.49 + 0.065|W| & \text{if } 8 \leq |W| \leq 22\ m\ s^{-1} \\ 1.2 & \text{if } 4 \leq |W| < 8\ m\ s^{-1} \\ 1.1 & \text{if } 1 \leq |W| < 4\ m\ s^{-1} \\ 2.6 & \text{if } |W| < 1\ m\ s^{-1} \\ 0.63 + 0.066|W| & \text{for all } |W| \\ 0.63 + (0.066|W|^2)^{1/2} & \text{for all } |W|. \end{cases}$$

This C_M formula follows Large and Pond [32] when the wind speed is less than $22\ m\ s^{-1}$; otherwise, it is assumed to be a constant as indicated in Powell et al. [12]. The equations (25) and (26) represent the surface boundary condition for the temperature and salinity equations (see the equations (27) and (28)). $\dot{T}$ represents the net surface heat flux and $\dot{S} \equiv S(0)[\dot{E} - \dot{P}]/\rho_\circ$ where $(\dot{E} - \dot{P})$ represents the net evaporation $\dot{E}$ – precipitation $\dot{P}$ fresh water surface mass flux rate and $S(0)$ represents the surface salinity.

2) Bottom boundary conditions:

$$w|_{-h} = -\left[u\frac{\partial h}{\partial x} + v\frac{\partial h}{\partial y}\right]_{-h} \quad (29)$$

$$A_{mv}\begin{bmatrix}\partial u/\partial z \\ \partial v/\partial z\end{bmatrix}_{-h} = \begin{bmatrix}\tau_{bx}/\rho_\circ \\ \tau_{by}/\rho_\circ\end{bmatrix} \quad (30)$$

$$\rho_\circ A_{hv}\frac{\partial T}{\partial z}\bigg|_{-h} = 0 \quad (31)$$

$$\rho_\circ A_{hv}\frac{\partial S}{\partial z}\bigg|_{-h} = 0 \quad (32)$$

The equation (29) represents the bottom boundary condition for the continuity equation (13), as expressed by the kinematic boundary condition. At the bottom, the kinematic boundary condition reflects the fact that there is no flow normal to the boundary, therefore, the material derivative $z + h$ is zero:

$$\frac{D(z + h)}{Dt} = \frac{Dz}{Dt} + \frac{Dh}{Dt} = 0 \implies$$

$$\left[\frac{\partial z}{\partial t} + u\frac{\partial z}{\partial x} + v\frac{\partial z}{\partial y} + w\frac{\partial z}{\partial z}\right]_{-h} + \left[\frac{\partial h}{\partial t} + u\frac{\partial h}{\partial x} + v\frac{\partial h}{\partial y}\right.$$

$$\left. + w\frac{\partial h}{\partial z}\right]_{-h} = 0 \quad (33)$$

and since, $\partial z/\partial t = \partial h/\partial t = \partial z/\partial x = \partial z/\partial y = \partial h/\partial z = 0$ and $\partial z/\partial z = 1$, the equation (33) reduces to the equation (29).

The equation (30) represents the bottom boundary condition for the z–momentum or the hydrostatic equation (16). The bottom shear stresses are parameterized as follows:

$$\begin{bmatrix}\tau_{bx} \\ \tau_{by}\end{bmatrix} = \rho_\circ C_D|u|\begin{bmatrix}u \\ v\end{bmatrix} \;\;; \;\; \tau_b = \rho_\circ C_D|u|u \;\;;$$

$$|u| = \left(u^2 + v^2\right)^{1/2} \quad (34)$$

where u and v are the horizontal flow velocities at the grid point closest to bottom and C_D is the bottom drag coefficient determined as the maximum between a value calculated according to the logarithmic law of the wall and a value equal to 0.0025:

$$C_D = \max\left[\mathbf{k}^2\left(\ln\frac{h + z_b}{z_\circ}\right)^{-2}, \; 0.0025\right] \quad (35)$$

where $z_\circ$ is the bottom roughness height in the present application $z_\circ = 1\ cm$, z_b is the grid point closest to bottom, and $\mathbf{k} = 0.4$ is the von Kármán's constant. In the 2D barotropic mode of the POM model, C_D is 0.0025.

On the side walls and bottom of the gulf, the normal gradients of T and S in the equations (31) and (32) are zero. Therefore, there are no advective and diffusive heat and salt fluxes across these boundaries.

3) Lateral boundary conditions: The GoT is modeled as a closed gulf without inflow or outflow from the gulf rivers. Consequently, the lateral conditions for a wall boundary are specified such that: (a) there is no flow normal to the wall ($\partial \mathbf{u}_n / \partial n = 0$), and (b) the no slip conditions tangential to the wall are valid ($\mathbf{u}_\tau = 0$), where $\mathbf{u}$ represents the velocity vector, and n and τ are the normal and tangential directions.

4) Wind stress and atmospheric pressure conditions: The typhoon pressure field and surface wind velocity created by the pressure gradient were modeled following the Bowden [10] and Pugh [29] relationships:

$$\frac{\partial p_{air}}{\partial \eta} = -\rho g, \tag{36}$$

$$\frac{\partial \eta}{\partial x} = \frac{\rho_{air} C_M W^2}{\rho g D}. \tag{37}$$

where p_{air} is the atmospheric pressure, η is the sea surface elevation from the reference level of undisturbed surface, ρ is the density of sea water in the z–momentum, g is the gravitational acceleration of the earth, x is the coordinate in the east–west direction, ρ_{air} is the density of air, C_M is the drag coefficient, W is the wind profile that results from the typhoon pressure gradient and D is the total depth of sea water. According to the equation (36), the pressure decreasing for 1 mb corresponds to about a 1 cm rise in sea level. The total water depth D inversely affects the sea surface elevation η, whereas the wind speed at the specific height (10 m) directly affects the sea surface elevation.

D. The numerical process of the WASS analyzed system

The numerical process of the WASS analyzed system is a non–staggered A–grid for the wave model (WAMC4) and a staggered C–grid for the hydrodynamic model (POM). For the WAMC4 model, the advection of wave energy is computed by using a forward in time, a first–order upwind differences (explicit) scheme in control volume form. The central differences are used to solve the spatial derivatives of u, v, and D in the equations (2)–(4) which the effect of current (u, v) on a staggered C–grid is neglected (see Fig. 1), and these terms are not computed at points beside the coast. It is worth noticing, u is the velocity in x–longitude direction, v is the velocity in y–latitude direction, and D is the total water depth ($D = \eta + H$) where η is the sea surface elevation and H is the local depth at the mean sea level (MSL). At this stage, the equation (1) is solved as an action conservation equation. The evolution of the source term S_{tot} is computed by a semi–implicit second order method (Leapfrog scheme). A limiter on the increments in wave energy is imposed (the discussion of Monbaliu et al. [9]). The spectrum F is represented by a discrete number of frequency bins, $\omega = 2\pi f$, traveling in a discrete number of directions, θ. The standard directional resolution is 30 degrees in 12 directions ($\Delta\theta = 30$), with an azimuthal distribution, whereas the discrete spectral space possesses 25 frequencies, ranging from 0.041Hz to 0.41Hz. A zero energy flux condition is imposed at coastlines and the possibility of imposing a time dependent condition at open boundaries is also included [34].
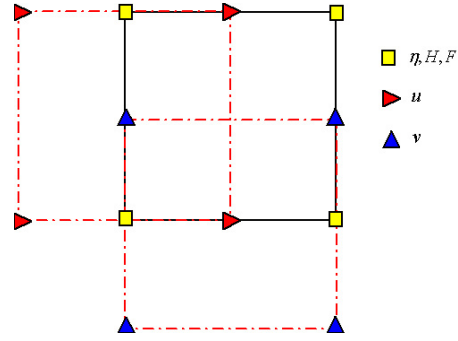

Fig. 1. Staggered C–type grid used by the hydrodynamic model. The wave model uses an nonstaggered A–type grid, in such a way that the governing equation for the wave evolution is computed at points corresponding to elevation values in the hydrodynamic model.

For the POM model, the computational stability condition on the external and internal modes was described by Worachat et al. [35]. The stability of both models was computed according to the Courant–Friedrichs–Lewy (CFL) stability condition. For more details of the sensitivity of the POM model to the time steps, see Ezer et al. [30].

III. MODEL PARAMETERS AND NUMERICAL EXPERIMENTS

The computational storm waves from the eye storm generated at the Pacific Ocean entering into the South China Sea (SCS) and the GoT were configured with high resolutions. In order to resolve the regional sea waves in the GoT and its surrounding water, the three nested domains (Fig. 2) with the fine grid domain (FGD) and the intermediate grid domain (IGD) imbedded into the coarse grid domain (CGD) by one way nested grid were employed in this study. The CGD was set up to cover the storm generations from $95°E$ to $155°E$ in longitude and from $20°S$ to $40°N$ in latitude ($0.5° \times 0.5°$ spatial grid size), which gave 121×121 points for both latitude and longitude. The IGD was covered from $98°E$ to $125°E$ in longitude and from $2°S$ to $25°N$ in latitude ($0.375° \times 0.375°$ spatial grid size), which gave 109×109 points for both latitude and longitude. The FGD was covered from $99°E$ to $111°E$ in longitude and from $2°N$ to $14°N$ in latitude ($0.25° \times 0.25°$ spatial grid size), which gave 49×49 points for both latitude and longitude. The propagation time steps of the CGD, IGD and FGD were 1,800, 1,200 and 600 s respectively while the source time steps of the CGD, IGD and FGD were also 1,800, 1,200 and 600 s respectively. All computational domains run under the deep water conditions with the spherical coordinates. The bottom topography was obtained from GEODAS (available online from http://www.ngdc.noaa.gov/mgg/gdas). The original version (1993), ETOPO5 [13], on a 5–minute latitude/longitude grid (1 minute of latitude = 1 nautical mile, or 1.853 km) was updated in June 2005 for the acceptably deep water. It was applied in the CGD in this study. The latest version (on July 28, 2008), ETOPO1 [2], on a 1–minute latitude/longitude grid for the high resolution was available in Ice Surface (top of Antarctic and Greenland ice sheets) and Bedrock (base of the ice sheets) versions. The ETOPO1 (Bedrock version) was chosen to apply in the FGD. The details

of the coupled topographies and nested grid domains were described by Xia et al. [14].

The WAMC4 model required the input wind fields and bathymetry data for each nested grid. The wind fields at a height of 10 m were obtained from the U.S. Navy Global Atmospheric Prediction System (NOGAPS) which is a global atmospheric forecasting model [31] with $1° \times 1°$ data resolution and the linear interpolation was used to generate the wind data to the grid points. The bathymetry data was extracted from ETOPO5 in the updated version and ETOPO1 [2].

For the POM model run in some parts of the SCS and GoT (see the FGD in Fig. 2) in the barotropic equation [1], the computations take place on a $0.1° \times 0.1°$ rectilinear horizontal grid and on a sigma vertical grid with 21 layers. The domain was covered from $99°E$ to $111°E$ in longitude and from $2°N$ to $14°N$ in latitude. The shoreline and the bathymetry of the GoT on the $0.1° \times 0.1°$ grid were obtained from ETOPO5 [13]. The forcing of model during the spin up period and the subsequent model simulations require the following meteorological data: temperature, salinity, sea level pressure, wind speed and direction. The wind and pressure fields were obtained from the U.S. Navy Global Atmospheric Prediction System (NOGAPS) which is a global atmospheric forecasting model with $1° \times 1°$ data resolution (Hogan and Rosmond [31]; Harr et al. [19]). The temperature and salinity with $1° \times 1°$ data resolution provided by Levitus94 (Levitus and Boyer [24]; Levitus et al. [23]) were indicated by the climatological monthly mean fields in the model. The high resolution of $0.1° \times 0.1°$ spatial grid size gave 121×121 points by using the bilinear interpolation of these data in the horizontal coordinate. In the vertical coordinate, 21 sigma levels were employed for adequacy and computational efficiency. The model time steps were $20\ s$ and $1200\ s$ (20 min) for the external and internal time steps respectively.

The results of WAMC4 and POM models were exposed in every hour of Typhoon Linda passing through the GoT. The stability of model was computed according to the CFL stability condition.

IV. RESULTS OF EXPERIMENTS

The computations of storm wave and coordinate propagation with the flag condition of the wave model, and the storm surge of the hydrodynamic model in the barotropic mode were analyzed. The numerical analysis of the significant wave height (Hs) generated by Typhoon Linda was firstly considered. The Hs related with the wind fields during the passage of Typhoon Linda in each domain is shown in Figs. (3)–(4). In the CGD, Super Typhoon Keith 1997 was also found in the Pacific Ocean while Typhoon Linda was in the SCS (Fig 3 (a)). Along the best track (Fig. 1), the FGD presented the wind field (Fig. 5(a)), wind stress and pressure drop (Figs. 5(b) and (c)) related with the Hs and sea surface elevation (Figs. 6(a) and (b)). The numerical simulations did not only presented the Hs and peak surge but also showed the coastal water level drop (Fig. 6(b)–(c)), and the energy loss of waves due to the bottom friction and percolation in the coastal zone (Fig. 4(c)).

The effects of the extreme Hs and sea surface elevation

and the difference between the maximum Hs and sea surface elevation computed by the WAMC4 and POM models at four locations of buoy (B1–B4) and ten locations of tide gauge station (S1–S10) in the GoT region (Fig 2(c) and Table I) were calculated. The differences of Hs and sea surface elevation at each station were presented in Table II. The results of the WAMC4 model showed that the Hs at B1, B2 and B3 were similarly different while at the station B4 showed a markedly different Hs. The results of the POM model showed that the maximum storm surge at each station presented the similar values and also showed the similar trends with the observational data, except those of the stations S5, S6 and S8.

V. CONCLUSION AND DISCUSSIONS

The results of both models are presented the incorporated surface wave in the regional zone affects into the coastal storm surge zone. Specifically, the results are indicated that the WASS generally under the approximation is not only the peak surge but also the coastal water level drop which can also cause substantial impact on the coastal environment. The wave–induced surface affected the storm surge can significantly improve storm surge prediction. Finally, the calibration of wave module according to the minimum error in the significant wave height (Hs) is not necessarily result in the optimum wave module in the WASS analyzed system for the WASS prediction. Additional studies will be investigated in the future with a focus on how waves and storm surges affect other domains in the GoT. The effects of wave and storm surge on the sea surface layer should be more comprehensively examined with more typhoon case simulations. Additionally, the observational data are needed to calibrate and validate with the harmonic analysis of tide in other models.

APPENDIX A
THE WAVE GROUP ON THE SPHERICAL EARTH

The great circle path of a wave group on the spherical earth may be written in the form :

$$\mathbf{x} = R\Big[\mathbf{e}_c \cos \frac{c_g t}{R} + \mathbf{e}_s \sin \frac{c_g t}{R}\Big], \qquad (38)$$

where R is the radius of the earth and c_g is the group velocity,

$$\mathbf{e}_c = \begin{cases} \cos \phi_0 \cos \lambda_0 \\ \cos \phi_0 \sin \lambda_0 \\ \sin \phi_0 \end{cases}, \qquad (39)$$

$$\mathbf{e}_s = \begin{cases} -\cos \theta_0 \sin \phi_0 \cos \lambda_0 + \sin \theta_0 \sin \lambda_0 \\ -\cos \theta_0 \sin \phi_0 \sin \lambda_0 - \sin \theta_0 \cos \lambda_0 \\ \cos \theta_0 \cos \phi_0 \end{cases}. \qquad (40)$$

The $\mathbf{e}_c$ and $\mathbf{e}_s$ are the orthogonal unit vectors pointing in the direction of the location and velocity, respectively. The wave group at time $t = 0$; λ_0, ϕ_0, θ_0 denotes the initial spherical coordinates and propagation direction. The vector $\mathbf{e}_s$ can be readily recognized as the wave group propagation direction by considering the special case $\lambda_0 = 0, \theta_0 = 0$ and then rotating the r–axis ($\theta_0 \neq 0$) and subsequently the z–axis ($\lambda_0 \neq 0$) to recover the general case.

The differential equation (38) with respect to t and setting $t = 0$ yields the propagation equations (2) and (3).

In addition, to derive the refraction equation (4), it is noted that

$$\cos\theta = \frac{1}{c_g}\left[\frac{d\mathbf{x}}{dt}\cdot\mathbf{e}_n\right], \qquad (41)$$

where

$$\mathbf{e}_n = \left\{ \begin{array}{c} -\sin\phi\cos\lambda \\ -\sin\phi\sin\lambda \\ \cos\phi \end{array} \right. , \qquad (42)$$

The $\mathbf{e}_n$ is the local northward–pointing horizontal unit vector. The differential equation (41) provides :

$$\frac{d\theta}{dt}\sin\theta = \frac{1}{c_g}\left[\frac{d^2\mathbf{x}}{dt^2}\cdot\mathbf{e}_n + \frac{d\mathbf{x}}{dt}\cdot\frac{d\mathbf{e}_n}{dt}\right] = \frac{1}{c_g}\frac{d\mathbf{x}}{dt}\cdot\frac{d\mathbf{e}_n}{dt}. \qquad (43)$$

which yields the equation (4) on substitution of the equations (38) and (2), (3) into $d\mathbf{x}/dt$ and $d\mathbf{e}_n/dt$. More discussions of the wave propagation on the spherical coordinate were given by the WAMDI Group [21].

References

[1] A. F. Blumberg and G. L. Mellor, A description of a three–dimensional coastal ocean circulation model, In N. S. Heaps, editor, Three–Dimensional Coastal Ocean Models, Coastal and Estuarine Sciences, American Geophysical Union, Washington, DC, 4(1987), 1–16.

[2] C. Amante and B. W. Eakins, 1 Arc–Minute Global Relief Model: Procedures, Data Sources and Analysis (ETOPO1), NOAA, National Geophysical Data Center, Boulder, Colorado, U.S.A. (2008), 21.

[3] G. J. Komen, K. Hasselmann and S. Hasselmann, On the existence of a fully developed windsea spectrum, Journal of Physical Oceanography, 14(1984), 1271–1285.

[4] G. Komen, L. Cavaleri, M. Donelan, K. Hasselmann, S. Hasselmann and P.A.E.M. Janseen, Dynamics and modelling of ocean waves, Cambridge University Press, UK. (1994), 532.

[5] G. L. Mellor, An equation of state for numerical models of oceans and estuaries, Journal of Atmospheric and Oceanic Technology, 8(1991), 609–611.

[6] G. Ph. van Vledder, Directional response of wind waves to turning winds, Commun. Hydraul. Geotech. Eng., Delft University of Technology, The Netherlands, 1990.

[7] H. Gunther, S. Hasselmann and P.A.E.M. Janssen, WAM model Cycle 4, Technical Report No. 4, Hamburg, Germany, 1992.

[8] H. L. Tolman, Wind wave propagation in tidal seas, Commun. Hydraul. Geotech. Eng., Delft University of Technology, The Netherlands, 1990.

[9] J. Monbaliu, R. Padilla–Hernandez, J. C. Hargreaves, J. C. Carretero–Albiach, W. Luo, M. Sclavo and H. Gunther, The spectral wave model WAM adapted for applications with high spatial resolution, Coastal Engineering, 41(2000), 4–62.

[10] K. F. Bowden, Physical oceanography of coastal waters, Ellis Horwood, Southampton, UK., (1983), 302.

[11] K. Hasselmann, T. P. Barnett, E. Bouws, H. Carlson, D. E. Cartwright, K. Enke, J. I. Ewing, H. Gienapp, D. E. Hasselmann, P. Kruseman, A. Meerbrug, P. Mauller, D. J. Olvers, K. Richter, W. Sell and H. Walden, Measurements of wind–wave growth and swell decay during the Joint North Sea Wave Project (JONSWAP), Deutsche Hydrographische Zeitschrift, 8(1973), 95.

[12] M. D. Powell, P. J. Vivkery and T. A. Reinhold, Reduced drag coefficient for high wind speeds in tropical cyclones, Nature, 422(2003), 278–283.

[13] M. O. Edwards, Global Gridded Elevation and Bathymetry on 5–Minute Geographic Grid (ETOPO5), NOAA, National Geophysical Data Center, Boulder, Colorado, U.S.A., 1989.

[14] M. Xia, L. Xie, L. J. Pietrafesa and M. Peng, A numerical study of storm surge in the cape fear river estuary and adjacent coast, Journal of Coastal Research, 24(2008), 159–167.

[15] N. Aschariyaphotha, P. Wongwises, S. Wongwises, U. W. Humphries and X. You, Simulation of seasonal circulations and thermohaline variabilities in the Gulf of Thailand, Advances in Atmospheric Sciences, 25(2008), 489–506.

[16] N. Booij, R. C. Ris, and L. H. Holthuijsen, A third–generation wave model for coastal regions Part 1, Model description and validation, Journal of Geophysical Research, 104(1999), 7649–7666.

[17] P.A.E.M. Janssen, Quasi–linear theory of wind–wave generation applied to wave forecasting, Journal of Physical Oceanography, 19(1991), 745–754.

[18] P. A. Wittmann and P. D. Farrar, Global, regional and coastal wave prediction, Marine Technology Society Journal, 31(1997), 76–82.

[19] P. Harr, R. Ellsberry, T. Hogan and W. Clune, North Pacific cyclone sea–level pressure errors with NOGAPS, Weather and Forecasting, 7(1992), 3.

[20] P. H. LeBlond and L. A. Mysak, Waves in the ocean. Elsevier, Amsterdam, 1978.

[21] S. Hasselmann, K. Hasselmann, E. Bauer, P.A.E.M. Janssen, G. J. Komen, L. Bertotti, P. Lionello, A. Guillaume, V. C. Cardone, J. A. Greenwood, M. Reistad, L. Zambresky and J. A. Ewing, The WAM model–a third generation ocean wave prediction model, Journal of Physical Oceanography, 18(1988), 1775–1810.

[22] S. Hasselmann, K. Hasselmann, J. H. Allender and T. P. Barnett, Computations and parameterizations of the nonlinear energy transfer in a gravity–wave spectrum, Part II: Parameterizations of the nonlinear energy transfer for application in wave models, Journal of Physical Oceanography, 15(1985), 1378–1391.

[23] S. Levitus, R. Burgett and T. Boyer, World Ocean Atlas: Salinity, NOAA Atlas NESDIS 3, U. S. Government Printing Office, Washington D.C., U.S.A., 3(1994b), 99.

[24] S. Levitus and T. Boyer, World Ocean Atlas: Temperature, NOAA Atlas NESDIS 4, U. S. Government Printing Office, Washington D.C., U.S.A., 4(1994a), 117.

[25] S. Vongvisessomjai, Impacts of Typhoon Vae and Linda on wind waves in the upper gulf of Thailand and east coast, Songklanakarin Journal of Science and Technology, 29(2007), 1199–1216.

[26] S. Vongvisessomjai, Tropical cyclone disasters in the Gulf of Thailand, Songklanakarin Journal of Science and Technology, 31(2009), 213–227.

[27] S. Vongvisessomjai, P. Chatanantavet and P. Srivihok, Interaction of tide and salinity barrier: Limitation of numerical model, Songklanakarin Journal of Science and Technology, 30(2008), 531–538.

[28] T. Brikshavana and A. Luadsong, Splitting modified Donor–Cell schemes for spectral action balance equation, International Journal of Computational and Mathematical Sciences, 4(2010), 214–222.

[29] T. D. Pugh, Tides, Surges and Mean Sea–Level, John Wiley & Sons, London, UK., (1987), 472.

[30] T. Ezer, H. Arango and A. F. Shchepetkin, Developments in terrain–following ocean models: intercomparison of numerical aspects, Ocean Modelling, 4(2002), 249–267.

[31] T. F. Hogan and T. E. Rosmond, The description of the Navy Operational Global Atmospheric System's spectral forecast model, Monthly Weather Review, 119(1991), 1786–1815.

[32] W. G. Large and S. Pond, Open ocean momentum fluxes in moderate to strong winds, Journal of Physical Oceanography, 11(1981), 324–336.

[33] W. Wannawong, U. W. Humphries and A. Luadsong, The application of curvilinear coordinate for primitive equation in the Gulf of Thailand, Thai Journal of Mathematics, 6(2008), 89–108.

[34] W. Wannawong, U. W. Humphries, P. Wongwises, S. Vongvisessomjai and W. Lueangaram, A numerical study of two coordinates for energy balance equations by wave model, Thai Journal of Mathematics, 8(2010), 197–214.

[35] W. Wannawong, U. W. Humphries, P. Wongwises, S. Vongvisessomjai and W. Lueangaram, Numerical modeling and computation of storm surge for primitive equation by hydrodynamic model, Thai Journal of Mathematics, 8(2010), 347–363.

Wiriya Lueangaram is a Commander and Water Expert at the Numerical Weather Prediction Center, Meteorological Division, Hydrographic Department, Royal Thai Navy, Thailand. His research interests involve numerical weather prediction, computational science, atmospheric modeling and oceanic modeling.
Email: viriya.navy@gmail.com

Worachat Wannawong received the B.Sc. degree in science-physics from Srinakharinwirot University, Bangkok, Thailand, in 2003, and the M.Sc. and Ph.D. degrees in applied mathematics from King Mongkut's University of Technology Thonburi (KMUTT), Bangkok, Thailand, in 2006 and 2010, respectively. He was with the Numerical Weather Prediction Center, Hydrographic Department, Royal Thai Navy from 2008 to 2010. He joined the Regional Ocean Modeling System (ROMS) team in October 2008. In April 2009, a part of his work was advised by Prof. Charitha Pattiaratchi and Prof. Krish Thiagarajan from the School of Environmental Systems Engineering and the School of Mechanical Engineering, University of Western Australia. In December 2009, he joined the workshop of the climate change project at KMUTT and Prof. Zhu Jiang from the Institute of Atmospheric Physics (IAP), Chinese Academy of Sciences, Beijing University gave him many ideas to modify the storm surge model by adjusting the drag coefficient. His research interests involve numerical analysis, numerical weather prediction, computational mathematics, and mathematical modeling.
Email: worachataj@hotmail.com

Usa W. Humphries received the B.Sc. degree in mathematics from Prince of Songkla University, Songkla, Thailand, in 1991, the M.Sc. degree in applied mathematics from KMUTT, in 1994, and the Ph.D. degree in applied mathematics from University of Exeter, England, in 2000. She was a National Research Council Postdoctoral Investigator with the James Rennell Division University of Southampton, Southampton, England, from November 2001 to December 2002 and with the IAP, China, from October 10 to November 10, 2005. She currently is an Associate Professor with the Department of Mathematics, KMUTT. Her research interests include numerical analysis, computational mathematics, oceanic modeling and climate change.
Email: usa.wan@kmutt.ac.th

Prungchan Wongwises received the B.Sc. (Second Honor) degree in mathematics from Chulalongkorn University, Bangkok, Thailand, in 1962, and the Diplom. Math. and Dr.rer.nat. degrees in mathematics from Technical University of Karlsruhe, Germany, in 1969 and 1974, respectively. She got the scholarships from the Technical University of Karlsruhe (Deutscher Akademischer Austauschdienst, DAAD), University of Freiburg, University of Kassel and University of Hannover under the German Government from 1966 to 1993. She currently is an Associate Professor with the Joint Graduate School of Energy and Environment, KMUTT. Her research interests include numerical analysis, computational mathematics, atmospheric modeling, oceanic modeling and air pollution modeling.
Email: prungchan.won@kmutt.ac.th

Suphat Vongvisessomjai is a Professor of Hydraulic and Coastal Engineering with the Water and Environment Expert, TEAM Consulting Engineering and Management Co., Ltd., Thailand. He was a lecturer in the Division of Water Resources Engineering, Asian Institute of Technology (AIT), Thailand, from 1968 to present and a project engineer in the Delft Hydraulics Laboratory, Netherlands, in 1980. He currently is a Professor and Director of Regional Environmental Management Center, Thailand. His research interests include drainage and flood control, coastal erosion and pollution, and water resources.
Email: suphat@team.co.th

TABLE I
THE OBSERVATIONAL AND COMPUTATIONAL POINTS FOR THE WAVE AND
HYDRODYNAMIC MODEL SIMULATIONS

Station code	Station name	Station point	Computational point
B1	Ko Chang	$102.20°E\ 12.00°N$	$102.25°E\ 12.00°N$
B2	Rayong	$101.22°E\ 12.44°N$	$101.25°E\ 12.50°N$
B3	Huahin	$100.17°E\ 12.44°N$	$100.25°E\ 12.50°N$
B4	Satun based weather	$101.42°E\ 9.28°N$	$101.50°E\ 9.25°N$
S1	Laem Ngob	$102.40°E\ 12.10°N$	$102.38°E\ 12.08°N$
S2	Laem Sing	$102.07°E\ 12.47°N$	$102.05°E\ 12.47°N$
S3	Prasae	$101.70°E\ 12.70°N$	$101.70°E\ 12.68°N$
S4	Rayong	$101.28°E\ 12.67°N$	$101.28°E\ 12.65°N$
S5	Tha Chin	$100.28°E\ 13.48°N$	$100.28°E\ 13.45°N$
S6	Mae Klong	$100.00°E\ 13.38°N$	$100.03°E\ 13.35°N$
S7	Pranburi	$99.98°E\ 12.40°N$	$100.10°E\ 12.40°N$
S8	Hua Hin	$99.97°E\ 12.57°N$	$99.95°E\ 12.57°N$
S9	Ko Lak	$99.82°E\ 11.80°N$	$99.84°E\ 11.78°N$
S10	Sichol	$99.90°E\ 9.00°N$	$99.92°E\ 8.98°N$

TABLE II
THE COMPARISON OF OBSERVATIONAL AND COMPUTATIONAL RESULTS

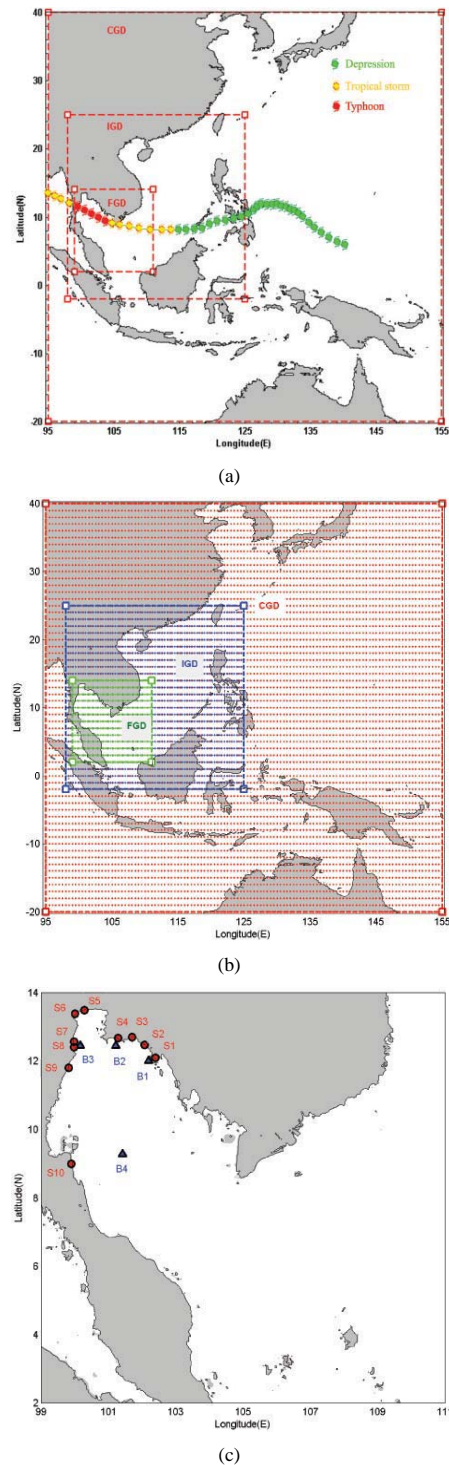| Station code	Station name	Observation (m)	Computation (m)
B1	Ko Chang	2.50	2.20
B2	Rayong	2.97	2.74
B3	Huahin	4.06	3.24
B4	Satun based weather	12.48	2.60
S1	Laem Ngob	1.18	0.24
S2	Laem Sing	1.23	0.28
S3	Prasae	1.34	0.29
S4	Rayong	1.18	0.33
S5	Tha Chin	2.08	0.44
S6	Mae Klong	1.96	0.46
S7	Pranburi	1.44	0.44
S8	Hua Hin	2.46	0.45
S9	Ko Lak	1.32	0.37
S10	Sichol	1.10	0.24

(a)

(b)

(c)

Fig. 2. Three pathway nested grids with the (a) typhoon track, (b) structural
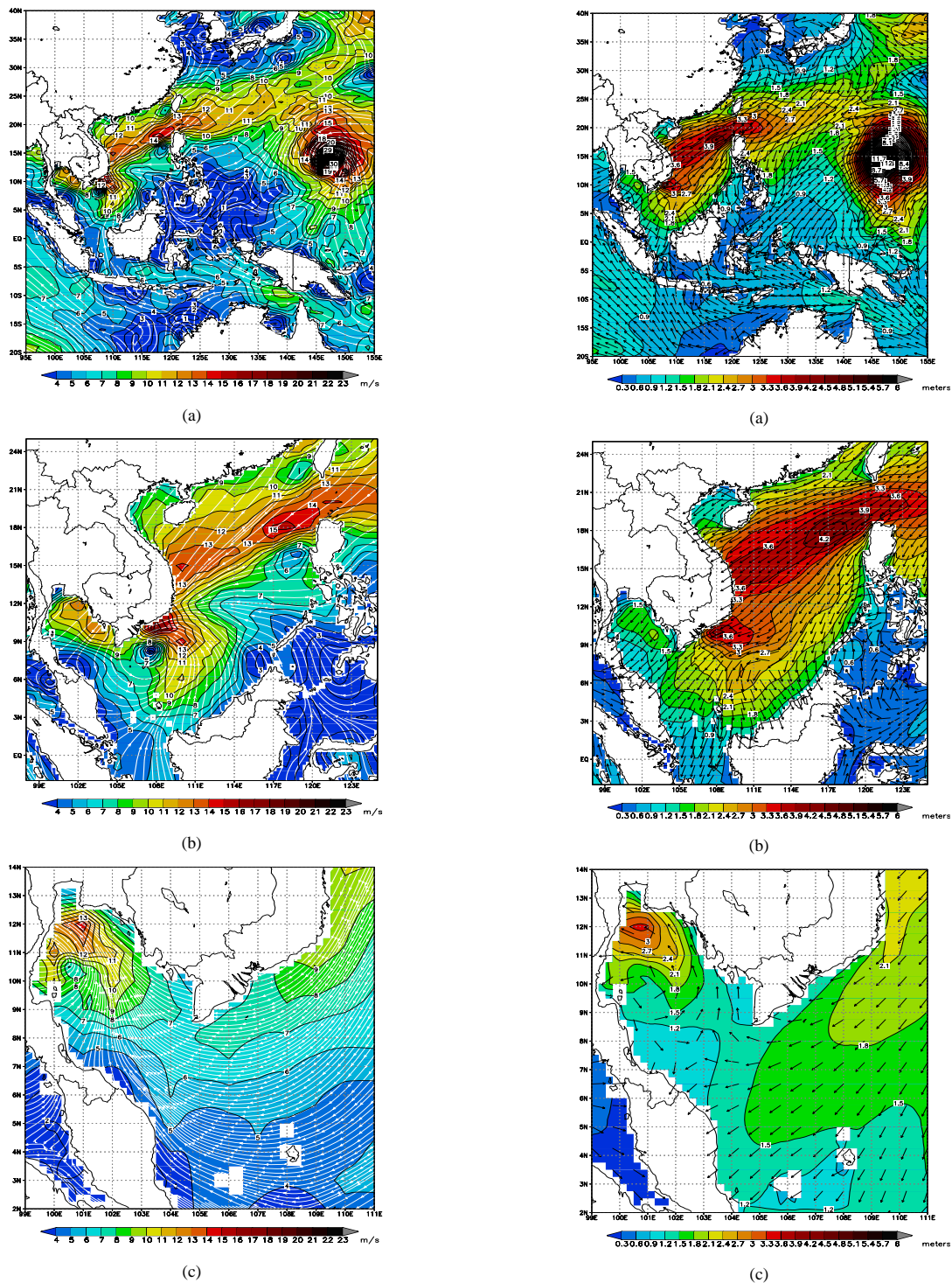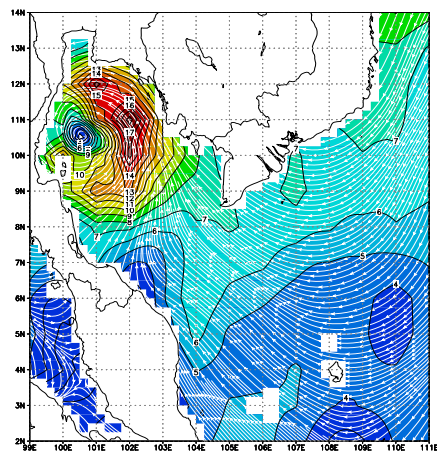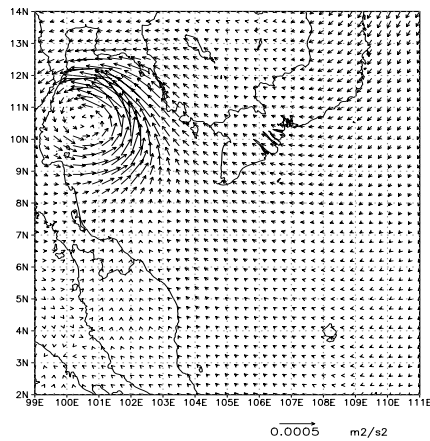grid resolution and (c) stations inside the FGD

Fig. 3.   Three pathway nested grids of wind streamline and speed (ms^{-1}) at (a) 23UTC01NOV1997 in the CGD, (b) 23UTC01NOV1997 in the IGD and (c) 19UTC03NOV1997 in the FGD
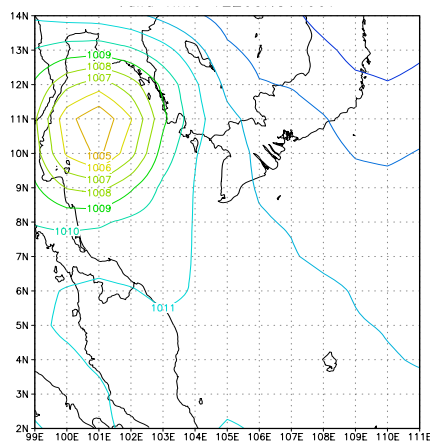
Fig. 4.   Three pathway nested grids of Hs (m) and direction at (a) 23UTC01NOV1997 in the CGD, (b) 23UTC01NOV1997 in the IGD and (c) 19UTC03NOV1997 in the FGD
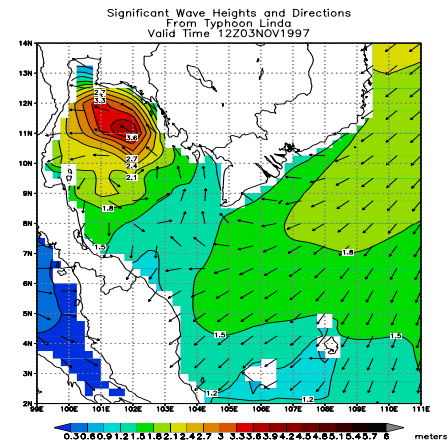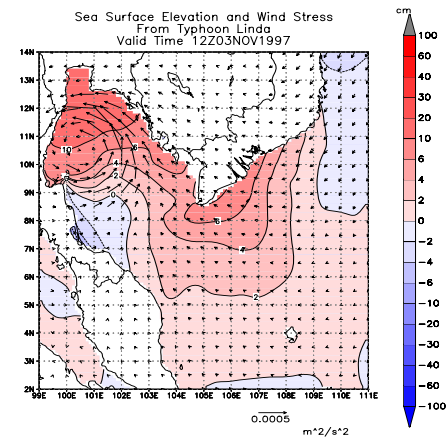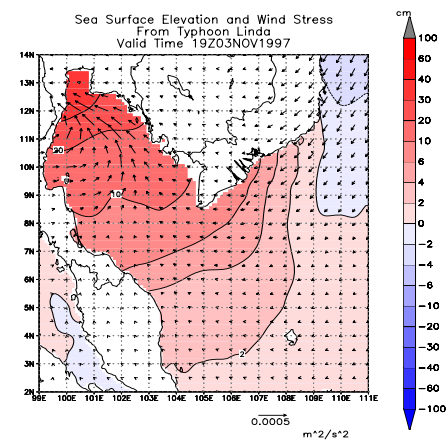
(a)

(b)

(c)

(a)

(b)

(c)

Fig. 5. (a) wind streamline and speed (ms^{-1}), (b) wind stress (Nm^2) and direction, and (c) sea level pressure (hPa) at 12UTC03NOV1997 in the domain (FGD)

Fig. 6. (a) Hs (m) and direction, (b) sea surface elevation (cm), wind stress (Nm^2) and direction at 12UTC03NOV1997, and (c) sea surface elevation (cm), wind stress (Nm^2) and direction at 19UTC03NOV1997 in the domain (FGD)